

Strongly coupled interface electronic states and interface phonon mode at GaP/Si(001)

Gerson Mette,¹ Kunie Ishioka,² Steven Youngkin,¹ Wolfgang Stolz,¹ Kerstin Volz,¹ and Ulrich Höfer¹

¹*Faculty of Physics and Materials Sciences Center,
Philipps-Universität Marburg, 35032 Marburg, Germany*

²*Nano-characterization Unit, National Institute for Materials Science, Tsukuba, 305-0047 Japan*
(Dated: May 9, 2023)

Ultrafast carrier and phonon dynamics at the buried heterointerface of GaP/Si(001) are investigated by means of two-color pump-probe reflectivity measurements. The carrier-induced reflectivity signal exhibits a resonant enhancement at pump-photon energies of 1.4 eV, which can be assigned to an optical transition between electronic interface states. The transient reflectivity is modulated by a coherent oscillation at 2 THz, whose amplitude also becomes maximum at 1.4 eV. The observed resonant behavior of the phonon mode in combination with a characteristic wavelength-dependence of, both, its frequency and initial phase, strongly indicate that the 2-THz mode is a difference-combination mode of a GaP-like and a Si-like phonon at the heterointerface and that this second-order scattering process can be enhanced by a double resonance involving the interfacial electronic states.

Coupling of charge and lattice degrees of freedom in semiconductors is one of the key factors to determine their crystalline structure and dominate the electronic, optical and thermal properties [1]. At surfaces of inorganic semiconductors, it has been established that the rearrangement of the atomic structure leads to well-defined electronic and phononic surface states [2]. In comparison, deeply buried interfaces have posed greater challenges due to the limitation of applicable experimental techniques and the complexity in theoretical simulations. Heterointerfaces between non-polar (e.g. Si) and polar (e.g. group III/V) semiconductors are particularly demanding, because of the possible localization of electric charges at the interface, the occurrence of anti-phase boundaries (APB), and because of the lattice mismatch between two semiconductors with different crystalline structures.

The interface of GaP and Si has recently gained attention because the two semiconductors have small mismatch in their lattice constants and can therefore serve as a template for Si-based III/V optoelectronics [3, 4]. To specify the atomic bonds and electric charges at the heterointerface, the growth of a pseudomorphic GaP nucleation layer on Si(001) was monitored *in situ* during the first growth steps by means of low-energy electron diffraction and reflection anisotropy spectroscopy, as well as simulated by density functional theory calculations [4–6]. The atomic structures of the interface and the APB were determined by transmission electron microscopy [3, 7] and cross-sectional scanning tunneling microscopy [8, 9]. Direct access to the *electronic* states at the buried interface has been limited, however, due to the small escape depth of photoelectrons in standard photoemission spectroscopy.

Nonlinear spectroscopic techniques such as second-harmonic generation (SHG) have advantages in their accessibility and sensitivity to buried interfaces. A previous time-resolved SHG study on a thin GaP nucleation layer on Si(001) revealed short-lived ($\lesssim 400$ fs) electronic

states that were resonantly excited at pump-photon energies of 1.4 eV [10]. This resonance was attributed to electronic states which are spatially localized at the heterointerface and which lie energetically in the band gap of the two semiconductors. This previous study observed no apparent lattice vibration, however, in spite of a general expectation for the emergence of interfacial phonon modes.

Transient reflectivity has been extensively applied to study carrier and phonon dynamics of semiconductor heterostructures [11, 12], though as a linear spectroscopic technique it has no specific sensitivity to interfaces or surfaces. In the present study, we investigate the interfacial carrier and phonon dynamics at GaP/Si(001) by performing transient reflectivity measurements using tunable near-infrared pump light. The carrier-induced reflectivity response from a thin GaP nucleation layer on Si(001) exhibits a clear resonance at 1.4 eV in agreement with the previous SHG measurements [10]. Moreover, the transient reflectivity signals are modulated by an oscillation at 2 THz, whose amplitude follows the same resonance as the carrier-induced response. The consistent resonant behavior unambiguously proves that this oscillation is an interface phonon mode. The observed wavelength-dependence of, both, frequency and initial phase of the 2-THz mode furthermore suggests that the interfacial phonon is enhanced by a double resonance involving the interface electronic states.

The studied sample is a nominally undoped 10-nm thick GaP nucleation layer grown at 450°C on *n*-type Si(001) by using flow-rate modulated metal-organic vapor phase epitaxy (MOVPE) [13, 14]. The GaP nucleation layer consists of crystalline grains with a lateral size of ≤ 30 nm as shown in Fig. S1 in the Supplementary Material (SM). Two-color pump-probe reflectivity measurements are performed under ambient conditions in the near back-reflection geometry. Two different sets of tunable femtosecond light sources are employed to cover the pump wavelength range of 720 – 1220 nm (photon energy

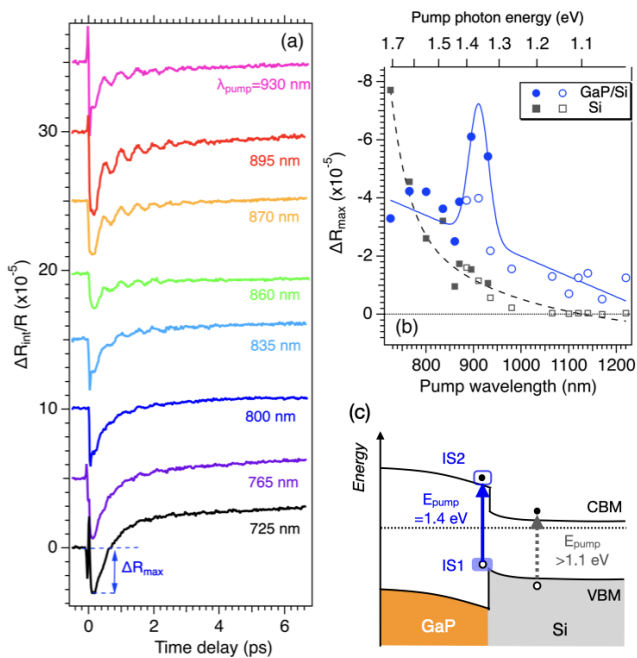


FIG. 1. (a) Interface-contribution in transient reflectivity of the GaP/Si heterostructure pumped at different wavelength and probed at 800 nm. Traces are offset for clarity. (b) Height of the initial drop R_{\max} of the interface contribution of GaP/Si as a function of the pump wavelength in comparison to bulk Si. Filled and open symbols are obtained with two different light sources. The latter are multiplied by 1.7 to scale to the former. Curves are to guide the eye. (c) Schematic band diagram of the GaP/Si interface. IS1 and IS2 indicate occupied and unoccupied interface states, respectively.

of 1.02–1.72 eV), whose details are described in Section II of the SM. The pump-photon energies are smaller than the indirect band gap of GaP (2.26 eV), but comparable with or larger than that of Si (1.12 eV). The probe wavelength was fixed at 800 nm (1.55 eV). The pump-induced change in the reflectivity $\Delta R/R$ is measured by detecting the probe lights before and after the reflection by the sample with a pair of matched photodiodes. The time delay t between the pump and probe pulses is scanned using a linear motor stage with slow scan technique.

The as-measured transient reflectivity signals ΔR from the GaP/Si sample (cf. Fig. S2(a) in the SM) contain contributions not only from the GaP overlayer/heterointerface ΔR_{int} but also from the Si substrate ΔR_{Si} . Therefore, we extract the former contribution by subtracting the latter from the as-measured signal ($\Delta R_{\text{int}} \equiv \Delta R - \Delta R_{\text{Si}}$) as described in more detail in Section III of the SM.

Fig. 1(a) compares the obtained overlayer/interface-contribution $\Delta R_{\text{int}}/R$ for different pump wavelengths. The transients show an abrupt drop at $t = 0$ which is followed by a double exponential increase. The height of the initial drop ΔR_{\max} , which gives a semi-quantitative measure for the photoexcited carrier density in the overlayer and at the heterointerface, exhibits a distinct resonance

peak at $\lambda_{\text{pump}} \simeq 900$ nm (photon energy of 1.4 eV) on top of the monotonic increase with decreasing wavelength (increasing pump-photon energy) as plotted in Fig. 1(b). As shown in the same figure, this resonance behavior is in apparent contrast to the initial drop height of bulk Si (c.f. Fig. S2(b) in SM for the corresponding transients of bulk Si). It coincides with the resonance of the fast SHG component obtained in our previous study on a thin ($d = 4.5$ nm) GaP film on Si(001) [10]. We therefore attribute the 1.4-eV resonance to an optical transition between interface electronic states as schematically shown in Fig. 1(c). After the initial abrupt drop, $\Delta R_{\text{int}}/R$ can be fitted to a multiple exponential function. The time constant for the fast rise is ~ 0.2 ps, which is comparable to the fast decay of the SHG signal observed previously [10]. The slower rise occurs on a similar time scale to that of bulk Si (cf. Fig. S2(b) in SM), ~ 40 ps, and is therefore attributed to the carriers photoexcited in the Si substrate and recombining at the GaP/Si interface [15–17].

The transient reflectivity signals of the GaP/Si sample also exhibit an apparent periodic modulation, as extracted in Fig. 2(a) after subtracting a multi-exponential baseline. This oscillation is not seen for bulk Si (Fig. S2(b) in SM) or bulk GaP (not shown) measured under the same conditions. Indeed, the frequency of this oscillation, 2 THz, has no counterpart in the previously reported first- and second-order Raman spectra of bulk GaP or Si [18, 19]. Hereafter we refer to the 2-THz oscillation as “low-frequency mode (LFM)”. In the fast Fourier-transform (FFT) spectra in Fig. 2(b), we also see a small overtone of the LFM at ~ 4 THz for $\lambda_{\text{pump}} < 800$ nm.

The oscillatory reflectivity in Fig. 2(a) can be fitted reasonably to a damped harmonic oscillation:

$$f(t) = A_{\text{LFM}} \exp(-\Gamma_{\text{LFM}} t) \sin(2\pi\nu_{\text{LFM}} t + \phi_{\text{LFM}}). \quad (1)$$

The fitting parameters A_{LFM} , Γ_{LFM} , ν_{LFM} and ϕ_{LFM} are plotted as a function of λ_{pump} in Figs. 2(c)-(e). The amplitude A_{LFM} in Fig. 2(c) exhibits a distinct resonant peak at $\lambda_{\text{pump}} \simeq 900$ nm (photon energy of 1.4 eV). This resonance behavior coincides with that of ΔR_{\max} in Fig. 1(b), indicating a strong coupling of the LFM with the interface electronic state. We therefore assign the LFM as an interface phonon mode coupled with the electronic transition at the GaP/Si interface. We note that the frequency ν_{LFM} [Fig. 2(d)] exhibits an apparent jump, whereas the initial phase ϕ_{LFM} [Fig. 2(e)] shows a shift by π , both, at $\lambda_{\text{pump}} \sim 800$ nm, which corresponds to our probe wavelength.

Phonons at semiconductor heterointerfaces have been studied extensively by means of resonant Raman scattering spectroscopy on GaAs/AlAs superlattices [20–26]. These studies reported higher-order (multiple) scattering in addition to the first-order scattering by a single phonon. The intensities of the higher-order Raman scattering were enhanced significantly by tuning the incident photon energy to, for example, the transition be-

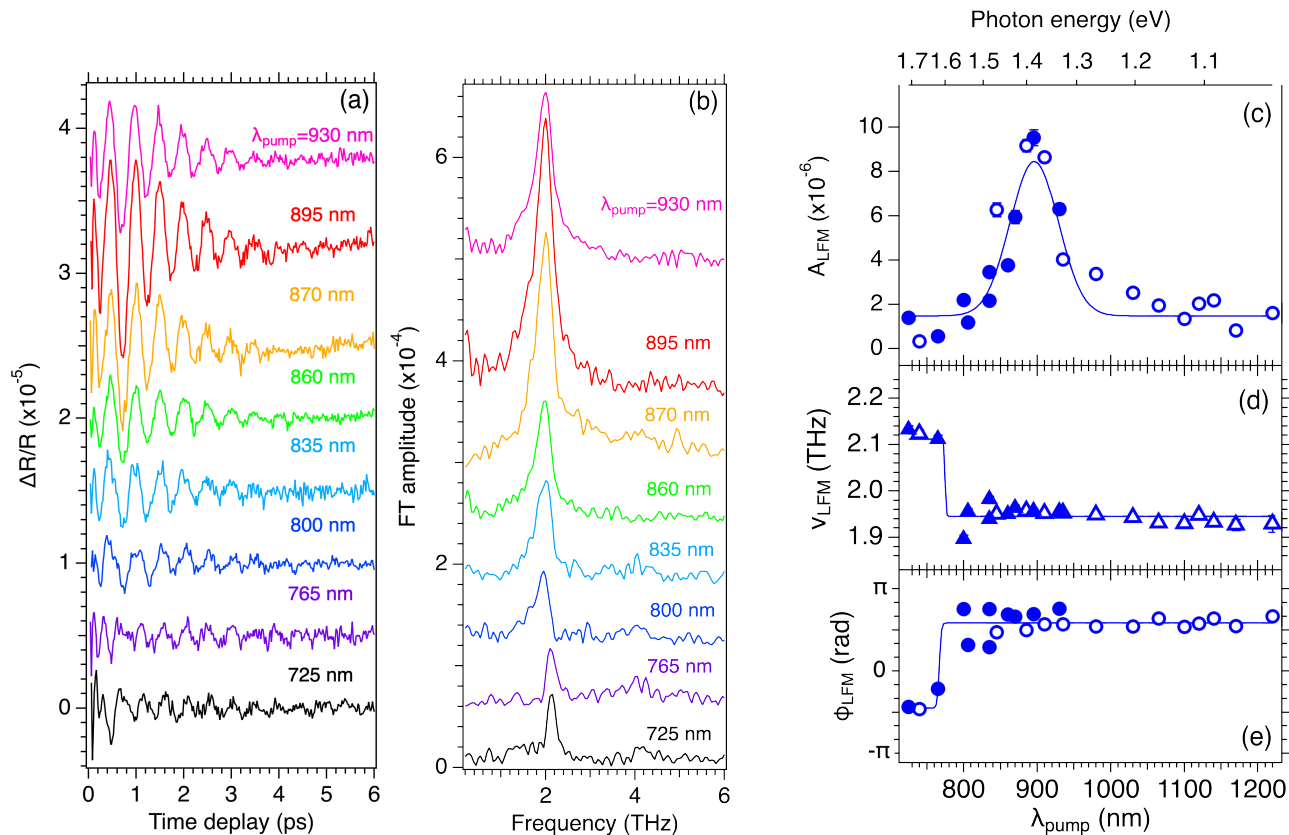


FIG. 2. (a) Oscillatory part of transient reflectivity of GaP/Si pumped at different wavelengths and (b) the corresponding fast Fourier transform (FFT) spectra. Traces are offset for clarity. (c) Amplitude, (d) frequency, and (e) initial phase of the low-frequency mode (LFM) as a function of the pump wavelength. Filled and open symbols in each panel represent the results obtained with two different light sources. In (c) the latter are multiplied by 1.7 to scale to the former. Curves are to guide the eye.

tween the sub-bands of a quantum well. Multiple scattering appeared not only by phonons within the same crystal, but also by those from two different materials, e.g. GaAs and AlAs. Whereas most of these studies focused on sum-combination modes appearing at high frequencies, there was also a report on a Raman peak appearing at low frequency of 108 cm^{-1} (3.2 THz) [25]. Based on its resonance behavior it was attributed to a difference-combination mode involving GaAs and AlAs optical phonons.

In the present study we similarly attribute the observed LFM to a difference-combination mode between GaP and Si optical phonons. The optical phonons of GaP and Si, both, reveal comparatively small dispersion along the $\Delta - X$ direction of the Brillouin zone as shown in Fig. 3b. Thus, there is relatively high density-of-states for a pair of Si and GaP optical phonons to satisfy energy and momentum conservation, i.e., $\nu_{\text{Si}} - \nu_{\text{GaP}} = 2 \text{ THz}$ and $\mathbf{k}_{\text{Si}} = -\mathbf{k}_{\text{GaP}}$. An exemplary second-order Raman scattering process that would give rise to the LFM is shown schematically in Fig. 3(b). It is initiated by the creation of electron-hole pairs upon optical excitation at the Γ -point, followed by the scattering of a Si

and a GaP optical phonon and finally terminated by the charge-carrier recombination.

In Fig. 2(d) and (e) we observed a small but clear discontinuity in the LFM frequency and a phase shift by π at $\lambda_{\text{pump}} \simeq \lambda_{\text{probe}}$. The phase shift is an indication for the Stokes and anti-Stokes processes in the short ($\lambda_{\text{probe}} < \lambda_{\text{pump}}$) and long ($\lambda_{\text{probe}} > \lambda_{\text{pump}}$) probe wavelength regimes, respectively [31]. In principle, Stokes and anti-Stokes scattering give rise to Raman peaks at the same frequency for first-order scattering by a zone-center phonon. But this is not necessarily the case for Raman scattering by zone-boundary phonons combined with double (or multiple) resonance. The frequency disparity between Stokes and anti-Stokes scattering was most famously demonstrated in the disorder-induced Raman bands (D , D' , D'' and their combination modes) of graphitic materials [32–35]. Correspondingly, a time-resolved study on graphene also reported a drastic frequency jump of the coherent D band at $\lambda_{\text{probe}} = \lambda_{\text{pump}}$ [36]. The frequency jump observed in the present study also occurs at $\lambda_{\text{probe}} \simeq \lambda_{\text{pump}}$, though not as drastic, and therefore can similarly be interpreted as a double resonance. Fig. 3(a) illustrates an example of a second-order

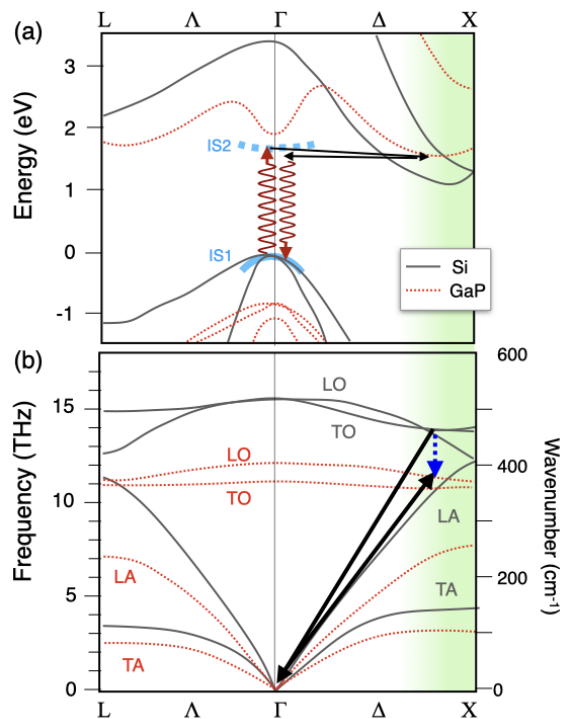


FIG. 3. (a) Schematic illustration of doubly resonant second-order Raman scattering at the GaP/Si interface (arrows). Calculated electronic structure of GaP [27] (orange curves) and Si [28] (gray curves) are superposed with a valence band offset of 0.8 eV. IS1 and IS2 indicate occupied and unoccupied interface states near the Γ -point, respectively. (b) Phonon dispersion curves of Si and GaP taken from Refs. [29, 30] with an example of a pair of Si and GaP optical phonons participating in the second-order scattering (arrows).

Stokes scattering with incoming resonance. Here the unoccupied interface state (IS2) and the GaP conduction band near the X -point contribute as the real intermediate states and thereby make the second-order scattering doubly resonant. The existence of such a double resonance can also explain the extraordinary large amplitude of the LFM near the electronic resonance at $E_{\text{pump}} = 1.4$ eV.

In conclusion, our two-color transient reflectivity measurements presented further experimental evidence for interface electronic states at the buried GaP/Si(001) heterointerface. In particular, an interface phonon mode was unambiguously resolved as a periodic modulation at ~ 2 THz, whose amplitude was resonantly enhanced by an electronic transition between the interface states. The oscillation was interpreted as a difference second-order Raman scattering involving a GaP and a Si optical phonon. The unusual photon-energy dependence of its frequency indicated the involvement of a multiple resonance. We thus demonstrated electron-phonon coupling that is characteristic to a heterointerface of polar and non-polar inorganic semiconductors, whose knowledge is indispensable in the construction of Si-based III/V optoelectronics.

ACKNOWLEDGMENTS

We gratefully acknowledge funding by the Deutsche Forschungsgemeinschaft (DFG, German Research Foundation), Project-ID 223848855-SFB 1083. The authors thank NIMS RCAMC and NAsP III/V GmbH for AFM measurements.

- [1] P. Y. Yu and M. Cardona, *Fundamentals of Semiconductors, 3rd ed.* (Springer, Berlin, 2005).
- [2] W. Mönch, *Semiconductor Surfaces and Interfaces* (Springer, Berlin, 2001).
- [3] A. Beyer and K. Volz, *Adv. Mater. Interfaces* **6**, 1801951 (2019).
- [4] O. Supplie, O. Romanyuk, C. Koppka, M. Steidl, A. Nägelein, A. Paszuk, L. Winterfeld, A. Dobrich, P. Kleinschmidt, E. Runge, and T. Hannappel, *Progress in Crystal Growth and Characterization of Materials* **64**, 103 (2018).
- [5] O. Supplie, M. M. May, G. Steinbach, O. Romanyuk, F. Grosse, A. Nägelein, P. Kleinschmidt, S. Brückner, and T. Hannappel, *J. Phys. Chem. Lett.* **6**, 464 (2015).
- [6] O. Romanyuk, O. Supplie, T. Susi, M. M. May, and T. Hannappel, *Phys. Rev. B* **94**, 155309 (2016).
- [7] A. Beyer, A. Stegmüller, J. O. Oelerich, K. Jandieri, K. Werner, G. Mette, W. Stolz, S. D. Baranovskii, R. Tonner, and K. Volz, *Chem. Mater.* **28**, 3265 (2016).
- [8] A. Lenz, O. Supplie, E. Lenz, P. Kleinschmidt, and T. Hannappel, *J. Appl. Phys.* **125**, 045304 (2019).
- [9] R. Saive, H. Emmer, C. T. Chen, C. Zhang, C. Honsberg, and H. Atwater, *IEEE J. Photovoltaics* **8**, 1568 (2018).
- [10] G. Mette, J. Zimmermann, A. Lerch, K. Brixius, J. Güdde, A. Beyer, M. Dürr, K. Volz, W. Stolz, and U. Höfer, *Appl. Phys. Lett.* **117**, 081602 (2020).
- [11] T. Dekorsy, G. Cho, and H. Kurz, Coherent phonons in condensed media, in *Light Scattering in Solids VIII*, Topics in Applied Physics, Vol. 76, edited by M. Cardona and G. Güntherodt (Springer, Berlin, 2000) p. 169.
- [12] M. Först and T. Dekorsy, Coherent phonons in bulk and low-dimensional semiconductors, in *Coherent Vibrational Dynamics*, Practical Spectroscopy, edited by S. D. Silvestri, G. Cerullo, and G. Lanzani (CRC, Boca Raton, 2007) pp. 130 – 172.
- [13] K. Volz, A. Beyer, W. Witte, J. Ohlmann, I. Nemeth, B. Kunert, and W. Stolz, *J. Crystal Growth* **315**, 37 (2011).
- [14] A. Beyer, J. Ohlmann, S. Liebich, H. Heim, G. Witte, W. Stolz, and K. Volz, *J. Appl. Phys.* **111**, 083534 (2012).
- [15] A. J. Sabbah and D. M. Riffe, *J. Appl. Phys.* **88**, 6954 (2000).
- [16] A. J. Sabbah and D. M. Riffe, *Phys. Rev. B* **66**, 165217 (2002).
- [17] K. Ishioka, E. Angerhoffer, C. J. Stanton, G. Mette, K. Volz, W. Stolz, and U. Höfer, *Phys. Rev. B* **105**,

- 035309 (2022).
- [18] R. Hoff and J. Irwin, *Can. J. Phys.* **51**, 63 (1973).
- [19] C. S. Wang, J. M. Chen, R. Becker, and A. Zdetsis, *Phys. Lett. A* **44**, 517 (1973).
- [20] M. H. Meynadier, E. Finkman, M. D. Sturge, J. M. Worlock, and M. C. Tamargo, *Phys. Rev. B* **35**, 2517 (1987).
- [21] V. V. Gridin, R. Beserman, and H. Morkoc, *Phys. Rev. B* **37**, 9061 (1988).
- [22] Z. V. Popovic, M. Cardona, E. Richter, D. Strauch, L. Tapfer, and K. Ploog, *Phys. Rev. B* **40**, 1207 (1989).
- [23] Z. V. Popovic, M. Cardona, E. Richter, D. Strauch, L. Tapfer, and K. Ploog, *Phys. Rev. B* **40**, 3040 (1989).
- [24] D. J. Mowbray, M. Cardona, and K. Ploog, *Phys. Rev. B* **43**, 11815 (1991).
- [25] J. Spitzer, I. Gregora, T. Ruf, M. Cardona, K. Ploog, F. Briones, and M. I. Alonso, *Solid State Commun.* **84**, 275 (1992).
- [26] S. L. Zhang, C. L. Yang, Y. T. Hou, Y. Jin, Z. L. Peng, J. Li, S. X. Yuan, and R. Planel, *J. Raman Spectroscopy* **27**, 249 (1996).
- [27] K. S. Sieh and P. V. Smith, *phys. stat. sol. b* **129**, 259 (1985).
- [28] K. Ishioka, K. Brixius, U. Höfer, A. Rustagi, E. M. Thatcher, C. J. Stanton, and H. Petek, *Phys. Rev. B* **92**, 205203 (2015).
- [29] W. Weber, *Phys. Rev. B* **15**, 4789 (1977).
- [30] P. H. Borchers, R. L. Hall, K. Kunc, and G. F. Alfrey, *J. Phys. C* **12**, 4699 (1979).
- [31] K. Mizoguchi, R. Morishita, and G. Oohata, *Phys. Rev. Lett.* **110**, 077402 (2013).
- [32] P. Tan, Y. Deng, and Q. Zhao, *Phys. Rev. B* **58**, 5435 (1998).
- [33] P. Tan, L. An, L. Liu, Z. Guo, R. Czerw, D. L. Carroll, P. M. Ajayan, N. Zhang, and H. Guo, *Phys. Rev. B* **66**, 245410 (2002).
- [34] L. Cancado, M. A. Pimenta, R. Saito, A. Jorio, L. Ladeira, A. Grueneis, A. Souza Fiho, G. Dresselhaus, and M. Dresselhaus, *Phys. Rev. B* **66**, 035415 (2002).
- [35] V. Zólyomi and J. Kürti, *Phys. Rev. B* **66**, 073418 (2002).
- [36] I. Katayama, K. Sato, S. Koga, J. Takeda, S. Hishita, H. Fukidome, M. Suemitsu, and M. Kitajima, *Phys. Rev. B* **88**, 245406 (2013).

Supplementary Material for Strongly coupled interface electronic state and interface phonon mode at GaP/Si(001)

Gerson Mette,¹ Kunie Ishioka,² Steven Youngkin,¹ Christopher J. Stanton,³ Wolfgang Stolz,¹ Kerstin Volz,¹ and Ulrich Höfer¹

¹*Faculty of Physics and Materials Sciences Center,
Philipps-Universität Marburg, 35032 Marburg, Germany*

²*Nano-characterization Unit, National Institute for Materials Science, Tsukuba, 305-0047 Japan*

³*Department of Physics, University of Florida, Gainesville, FL 32611 USA*

(Dated: May 9, 2023)

I. SAMPLE FABRICATION AND CHARACTERIZATION

The studied GaP/Si heterostructure sample consists of a nominally undoped GaP film with a nominal thickness of $d=10$ nm which is grown on an exact Si(001) substrate by metal-organic vapor phase epitaxy (MOVPE) [1, 2]. First, a homoepitaxial Si-buffer layer is deposited on an n-type ($\rho = 0.007 - 0.02\Omega\text{cm}$) Si(001) substrate with a 0.23° intentional miscut in [110]-direction, and annealed in H_2 atmosphere to stabilize double steps. A thin GaP nucleation layer is then grown on the Si substrate by flow-rate modulated epitaxy (FME) at 450°C , where the Ga and P precursors are injected intermittently. The as-grown GaP nucleation layer consists of crystalline grains with a lateral size of ≤ 30 nm as shown in Fig. S1.

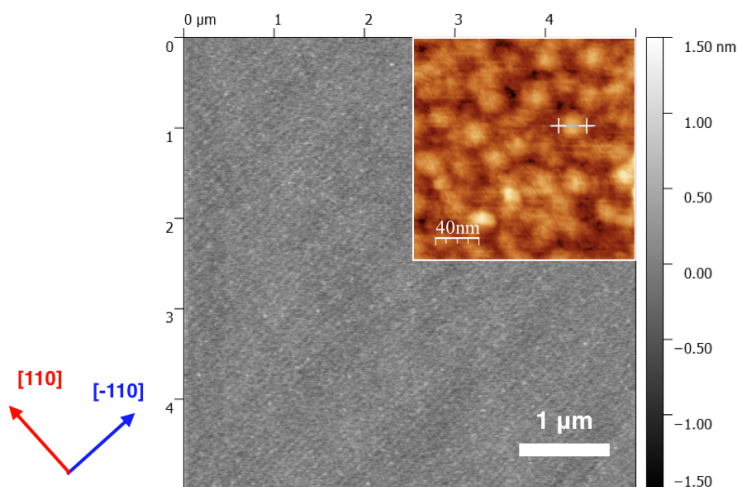


FIG. S1. Atomic force microscopy image of the 10-nm thick GaP nucleation layer on Si(001).

II. SPECTROSCOPIC EXPERIMENTAL METHODS

Two-color pump-probe reflectivity measurements are performed under ambient conditions using two different sets of light sources to cover the pump wavelength range of 720 – 1220 nm (photon energies of 1.02 – 1.72 eV). On the one hand, the output of a non-collinear optical parametric amplifier (Orpheus-N-2H, LightConversion) with tuneable wavelength range between 720 and 920 nm (photon energies of 1.35 – 1.72 eV), 30-fs pulse duration and 200-kHz repetition rate is mainly used as pump beam, whereas the output of an Orpheus-F-TWIN (LightConversion) at 800 nm (1.55 eV photon energy), 40-fs duration and 200-kHz repetition rate is used as probe beam. On the other hand, to cover the longer pump wavelength, the idler output of a collinear optical parametric amplifier (OPA 9450, Coherent) with tuneable wavelength range between 845 and 1220 nm (photon energies of 1.02 – 1.47 eV), 50-fs pulse duration and 100-kHz repetition rate is used as pump beam, whereas the output of a regenerative amplifier (RegA 9050, Coherent) with 800-nm center wavelength, 50-fs duration and 100-kHz repetition rate is used as probe beam. The photon energies employed in the present study are lower than the indirect bandgap of GaP (2.26 eV) or the direct gap of Si (3.4 eV) but comparable with or larger than the indirect gap of Si (1.12 eV).

The linearly polarized pump and probe beams are focussed to a $\sim 30\text{-}\mu\text{m}$ diameter spot on the sample surface in the near back-reflection geometry, with incident angles of $\lesssim 15^\circ$ and $\lesssim 5^\circ$ from the surface normal. Incident pump and probe densities correspond to 4 and 0.7 mJ/cm^2 . The pump-induced change ΔR in the reflectivity R is measured by detecting the probe lights before and after the reflection by the sample (isotropic detection) with a pair of matched Si PIN photodiodes. The pump beam is chopped at around 2 kHz for lock-in detection. The time delay t between the pump and probe pulses is scanned using a linear motor stage with a slow scan technique.

III. SUBTRACTION OF THE SI CONTRIBUTION FROM THE AS-MEASURED TRANSIENT REFLECTIVITY

The as-measured transient reflectivity signals from the GaP/Si sample, plotted in Fig. S2a, contain contributions from the GaP overlayer and the heterointerface (ΔR_{int}) as well as from the Si substrate (ΔR_{sub}). We extract the former contribution by subtracting the latter from the as-measured signal ΔR as follows:

$$\frac{\Delta R_{\text{int}}(t)}{R_0} \equiv \frac{\Delta R(t)}{R_0} - \frac{\Delta R_{\text{sub}}(t)}{R_0}. \quad (\text{S1})$$

The resulting transients are shown in Fig. 1a in the main text for different pump wavelengths.

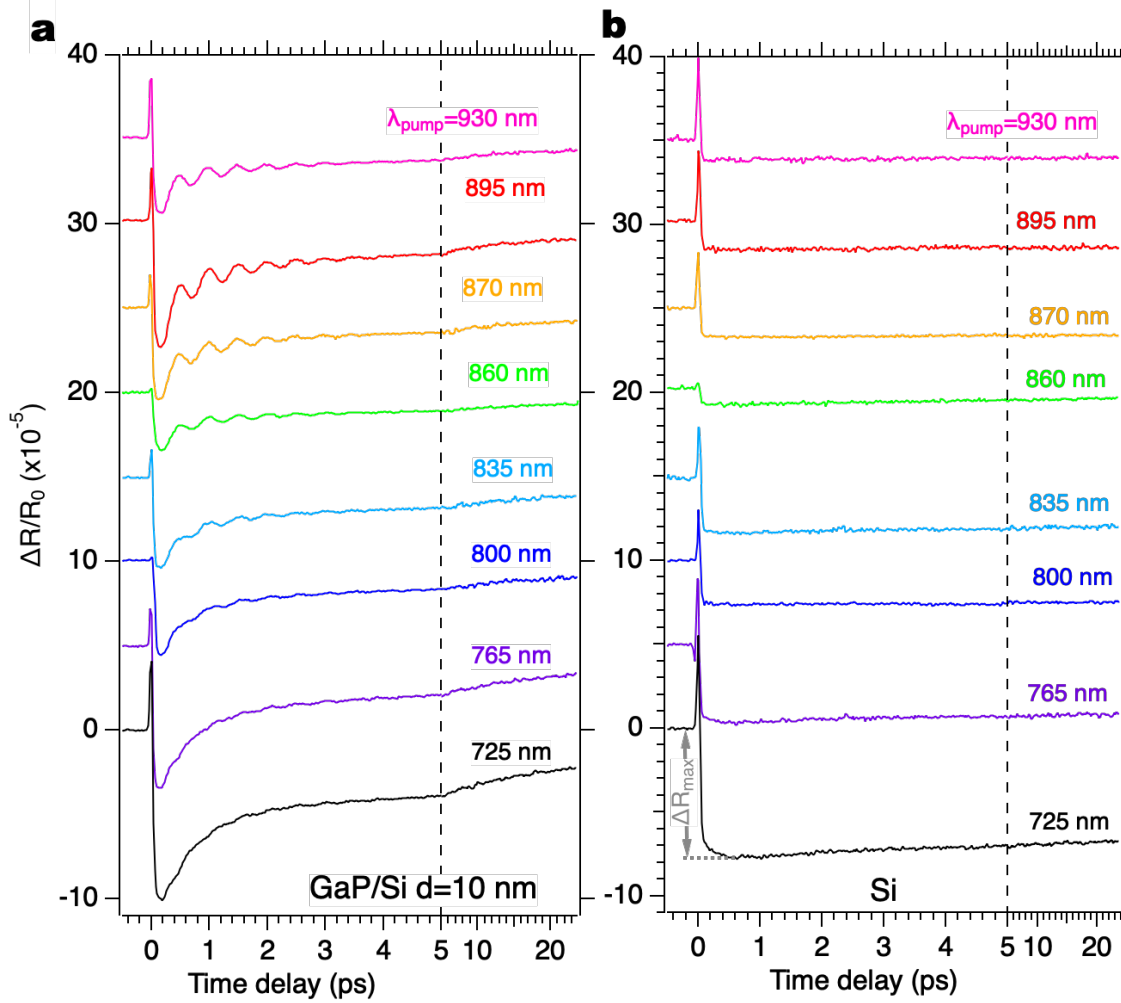


FIG. S2. As-measured transient reflectivity signals of the GaP/Si sample (a) and of Si without a GaP overlayer (b) pumped at different wavelengths and probed at 800 nm. The arrow in (b) indicates the initial step height ΔR_{max} for Si. Traces are offset for clarity.

In Eq. (S1) the contribution from the Si substrate depends on the overlayer thickness d , the pump wavelength λ_{pump} and the probe wavelength λ_{probe} due to interferences at the heterointerface. As discussed in detail in Ref. [3], it can be approximately given by:

$$\frac{\Delta R_{\text{sub}}(t, d)}{R_0} \equiv \frac{T_0(d, \lambda_{\text{pump}})P_2(d, \lambda_{\text{probe}})}{T_0(0, \lambda_{\text{pump}})P_2(0, \lambda_{\text{probe}})} \frac{\Delta R_{\text{Si}}(t)}{R_0}, \quad (\text{S2})$$

using the transient reflectivity of Si without GaP overlayer measured at the same condition, $\Delta R_{\text{Si}}(t)$, which is shown in Fig. S2b. $P_2(d, \lambda_{\text{probe}})$ in Eq. (S2) represents the change in the reflected probe light intensity due to a pump-induced disturbance in the refractive index n_2 of the Si substrate:

$$\begin{aligned} P_2(d, \lambda_{\text{probe}}) &\equiv \frac{1}{R_0(d, \lambda_{\text{probe}})} \frac{\partial R_0}{\partial r_{12}} \frac{\partial r_{12}}{\partial n_2} \\ &= \frac{2r_{12}(1 - r_{01}^4) + 2r_{01}(1 + r_{12}^2)(1 - r_{01}^2) \cos 2(n_1 k_0 d)}{(r_{01}^2 + r_{12}^2 + 2r_{01}r_{12} \cos 2n_1 k_0 d)(1 + r_{01}^2 r_{12}^2 + 2r_{01}r_{12} \cos 2n_1 k_0 d)} \times \frac{-2n_1}{(n_1 + n_2)^2}. \end{aligned} \quad (\text{S3})$$

where R_0 denotes the reflectance of the heterointerface at wavelength λ and wavevector $k_0 = 2\pi/\lambda$ in air:

$$R_0(d, \lambda) = \left| \frac{r_{01} + r_{12} e^{4i\pi n_1 k_0 d / \lambda}}{1 + r_{01} r_{12} e^{4i\pi n_1 k_0 d / \lambda}} \right|^2. \quad (\text{S4})$$

r_{01} and r_{12} are the reflection coefficients for the light waves incoming from air into GaP and from GaP into Si:

$$r_{01} = \frac{1 - n_1}{1 + n_1}; \quad r_{12} = \frac{n_1 - n_2}{n_1 + n_2}, \quad (\text{S5})$$

with n_1 and n_2 being the refractive indices of GaP and Si. T_0 in eq. (S2) represents the transmittance of the heterointerface, i.e., the pump intensity penetrating into the Si substrate:

$$T_0(d, \lambda_{\text{pump}}) = 1 - R_0(d, \lambda_{\text{pump}}) = \frac{(1 - r_{01}^2)(1 - r_{12}^2)}{1 + r_{01}^2 r_{12}^2 + 2r_{01}r_{12} \cos 2n_1 k_0 d}. \quad (\text{S6})$$

[1] K. Volz, A. Beyer, W. Witte, J. Ohlmann, I. Nemeth, B. Kunert, and W. Stolz, *J. Crystal Growth* **315**, 37 (2011).

[2] A. Beyer, J. Ohlmann, S. Liebich, H. Heim, G. Witte, W. Stolz, and K. Volz, *J. Appl. Phys.* **111**, 083534 (2012).

[3] K. Ishioka, E. Angerhoffer, C. J. Stanton, G. Mette, K. Volz, W. Stolz, and U. Höfer, *Phys. Rev. B* **105**, 035309 (2022).